MATERIALS CHEMISTRY FRONTIERS

RESEARCH ARTICLE

View Article Online
View Journal | View Issue

Cite this: *Mater. Chem. Front.*, 2023, 7, 3398

Peripheral engineering of platinum(II) dicarbene pincer complexes for efficient blue hyperphosphorescent organic light-emitting diodes†

Ze-Lin Zhu, ‡*[a] Jie Yan,‡[b] Li-Wen Fu,[c] Chen Cao,[a] Ji-Hua Tan,[a] Sheng-Fu Wang,[c] Yun Chi *[ab] and Chun-Sing Lee *[a]

Received 17th March 2023,
Accepted 9th May 2023

DOI: 10.1039/d3qm00273j

rsc.li/frontiers-materials

Pt(II) dicarbene pincer complexes have been explored as deep-blue phosphors with narrowband emissions. Generally, they form excimers easily and their relatively long emission lifetimes also limit their applications as OLED emitters. Herein, we developed a simple method to modify 1,3-bisimidazol-3-ium pro-chelates and obtained three Pt(II) dicarbene pincer complexes, thus studying the issue of excimer formation *vs.* peripheral appendages. As a result, blue emissions can be maintained at doping concentrations of up to 20 wt% for IPr*t*BuPt. Moreover, the emission of IPr*t*BuPt was found to significantly overlap with the absorption of ν-DABNA, an efficient blue boron/nitrogen based multi-resonant TADF molecule. A hyper-OLED using IPr*t*BuPt as a sensitizer and ν-DABNA as a terminal emitter achieved EQEs of up to 33.59%, FWHM of 20 nm and CIE coordinates of (0.124, 0.148). These results demonstrated a successful example of utilizing both structural engineering and smart device architecture for getting efficient blue devices with suppressed efficient roll-off.

Introduction

While there has been significant progress in the utilization of both red and green phosphors for fabrication of organic light-emitting diodes (OLEDs),[1–5] the development of blue phosphors is significantly delayed. Therefore, blue fluorophores, which can only utilize one quarter of electrogenerated excitons, are still being used in modern commercial OLED products.[6] Thus, novel blue emitters and device architectures are urgently needed for boosting the performance of blue OLED devices.[7,8]

Multi-resonant thermally activated delayed fluorescent (MR-TADF) molecules have become the most intensively researched topics due to their merits including fast radiative decay,[9–11] narrow full width at half maximum (FWHM), proneness to adapt horizontal alignment and high luminescent efficiency.[12,13] Thus, MR-TADF molecules possess great potential to improve external quantum efficiency (EQE) towards 40% with color purity comparable to quantum dot LEDs,[14–17] simultaneously. Another type of promising emitter is an N-heterocyclic carbene (C^C_{NHC}) coordinated iridium(III) complex (Ir(C^C_{NHC})$_3$),[18] a representative emitter of which, *i.e.*, *mer*-Ir(CF_3pbp)$_3$, has delivered an EQE_{max} of 21.2% with Commission Internationale de L'Eclairage (CIE) coordinates of (0.16, 0.05),[19] showing performances comparable to the state-of-the-art TADF emitters. This result is ascribed to the strong σ-donating C^C_{NHC} chelate, which greatly destabilizes the metal-centered (MC) dd excited state and enlarged energy offset between the emitting excited states and upper lying MC dd quenching states.[7,8]

Compared to TADF emitters and Ir(III) complexes, the development of deep-blue Pt(II) complexes is relatively lagging behind. In fact, the large spin-orbital coupling (SOC) constant of the Pt atom (4881 *vs.* 3450 cm^{-1} for Ir)[20] confirmed its potential for achieving efficient phosphorescence. Incorporating an N-heterocyclic carbene entity, Li *et al.* demonstrated a tetradentate N^C^C^C_{NHC} coordinated Pt(II) complex with an EQE_{max} of 24.8% and CIE coordinates of (0.148, 0.079).[21,22] However, its square-planar geometry and long radiative lifetime resulted in a low luminance and increased efficiency roll-off at high luminance (*e.g.*, 1000 cd m^{-2}). Modifications to alleviate this problem are impeded by the sophisticated synthetic procedure of

[a] *Center of Super-Diamond and Advanced Films (COSDAF) and Department of Chemistry, City University of Hong Kong, Hong Kong SAR, China. E-mail: zelinzhu-c@my.cityu.edu.hk, apcslee@cityu.edu.hk*
[b] *Department of Materials Science and Engineering, City University of Hong Kong, Hong Kong SAR, China. E-mail: yunchi@cityu.edu.hk*
[c] *Department of Chemistry and Frontier Research Center on Fundamental and Applied Sciences of Matters, Tsing Hua University, Hsinchu 30013, Taiwan, China*

† Electronic supplementary information (ESI) available. CCDC 2247274-(MeCF3Pt), 2247257(IPrCF3Pt) and 2247276(IPr*t*BuPt). For ESI and crystallographic data in CIF or other electronic format see DOI: https://doi.org/10.1039/d3qm00273j

‡ Equally contributed.

tetradentate chelates.[23,24] In contrast, the dicarbene pincer chelate can be modified much more easily. A pioneering research study shows a decent blue emission with a narrow FWHM down to ~20 nm and a blue device with an EQE_{max} of 14.8% and CIE coordinates of (0.16, 0.13) using Pt(II) based C_{NHC}^C^C_{NHC} pincer complexes as dopants,[25,26] although they gave dimers (or excimers) at higher doping ratios. On the other hand, lowered doping ratios may lead to unbalanced transport of carriers, which undermine device performance at high brightness (*e.g.*, 100 and 1000 cd m^{-2}). In fact, the emission of our Pt(II) pincer complexes exerts good spectral overlaps with absorption bands of the blue terminal emitter, *i.e.*, ν-DABNA (N^7,N^7,N^{13},N^{13},5,9,11,15-octaphenyl-5,9,11,15-tetrahydro-5,9,11,15-tetraaza-19*b*,20*b*-diboradinaphtho [3,2,1-*de*:1′,2′,3′-*jk*]pentacene-7,13-diamine).[15] This encouraged us to employ the Förster resonance energy transfer (FRET) process in realizing efficient blue OLEDs.[27–29]

Herein, we modify the peripheral groups of the C_{NHC}^C^C_{NHC} chelate to minimize intermolecular interactions and to develop three Pt(II) (C_{NHC}^C^C_{NHC}) pincer complexes, namely MeCF3Pt, IPrCF3Pt and IPr*t*BuPt. These modifications have successfully addressed the issue on excimer formation and given pure blue emission with EQE_{max} = 13.96% and CIE coordinates of (0.159, 0.241) from an IPr*t*BuPt-based OLED device. More importantly, the emission of IPr*t*BuPt shows a significant overlap with the absorption of MR-TADF blue emitter – ν-DABNA. A hyperphosphorescent device with IPr*t*BuPt as a dopant sensitizer and ν-DABNA as a terminal emitter is demonstrated to show a maximum EQE of 33.59% and color coordinates of (0.124, 0.148). It also revealed very mild efficiency roll-offs comparable to other hyper-OLED devices in the literature,[7,8,15,23,24,30–38] together with a high max. brightness of ~30 000 cd m^{-2}. Eventually, this study shows that a combination of simple structural modifications of Pt(II) dicarbene pincer complexes and smart device engineering can be promising in the generation of high performance blue OLEDs.

Results and discussion

Synthesis of the dicarbene pincer pro-chelates follows the same protocol reported in our previous works.[39,40] The Pt(II) complexes are obtained by refluxing K_2PtCl_4 and hexafluorophosphate salts of their corresponding 1,3-bisimida-zol-3-ium pro-chelates (Scheme 1 and the Experimental section) in the presence of potassium carbonate in propionic acid (yield: 34–54%, Scheme 1). It is noted that this method is simpler and more straightforward than the other literature precedents, which needs expensive reagents and afforded low product yields (<10%).[25,26] Finally, all products were characterized using ^1H and ^{19}F NMR spectroscopies, high-resolution mass spectrometry (HR-MS), and single-crystal X-ray crystallographic analysis.

UV-Vis absorption spectra of these Pt(II) complexes show two main absorption bands (Fig. 1), namely π–π* absorption of the aromatic entities at ~320 nm and the mixed ligand-centered π–π* absorption and metal-to-ligand charge transfer (MLCT) at the region ≥330 nm. Compared to the CF_3-substituted complexes

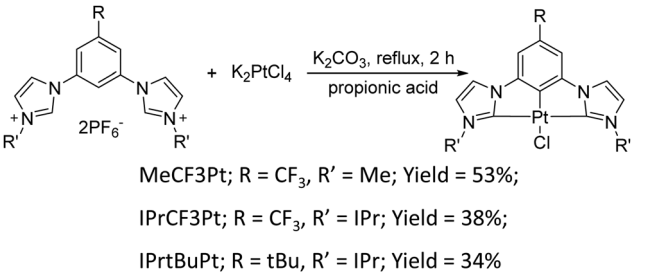

Scheme 1 Synthetic route and chemical structures of MeCF3Pt, IPrCF3Pt and IPr*t*BuPt.

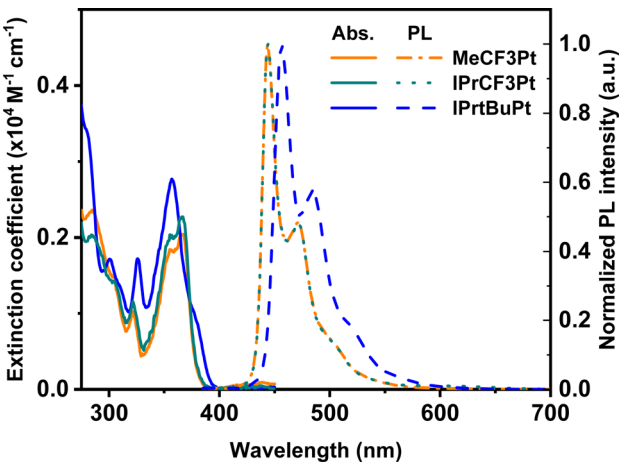

Fig. 1 Normalized UV-vis absorption (solid) and emission (dashed) spectra of the new Pt(II) complexes in DCM solution.

(MeCF3Pt and IPrCF3Pt), *t*Bu-substituted IPr*t*BuPt presents a slightly redshifted absorption peak (Table 1) and decreased MLCT intensity, implying a smaller energy gap and less MLCT involvement in transition. Thus, the substitution of the electron-rich group at the benzene ring will reduce the mix between the π* orbital of the ligand and dπ orbital of the metal center.[41] Consistently, a slightly redshift emission in IPr*t*BuPt (458 *vs.* 444 nm) with an enhanced 0–1 transition band (FWHM increases from 16 to 44 nm, ascribed to a greater contribution from ligand-centred π–π* transition)[42] is observed in the photoluminescent (PL) spectrum in CH_2Cl_2 solution (10^{-5} M). Concomitantly, the longest radiative lifetime (7.84 μs) is observed from IPr*t*BuPt. Isopropyl substituents in IPrCF3Pt and IPr*t*BuPt introduce an extra vibrational degree of freedom to the molecule and result

Table 1 Photophysical data of the Pt(II) complex in DCM (10^{-5} M)

Name	λ_{Abs}[a] [nm]	λ_{em}[a] [nm]	PLQY[ab] [%]	FWHM[a] [nm]	τ[a] [ns]
MeCF3Pt	320, 356, 367	444, 471	73.2	16	3187
IPrCF3Pt	320, 356, 367	444, 471	46.4	16	2334
IPr*t*BuPt	326, 357, 376 (sh)	458, 485	46.7	44	3660

[a] Measured in degassed DCM. [b] Coumarin 102 (C102) in MeOH (10^{-5} M, Q.Y. = 87% and λ_{max} = 480 nm) was employed as the standard.

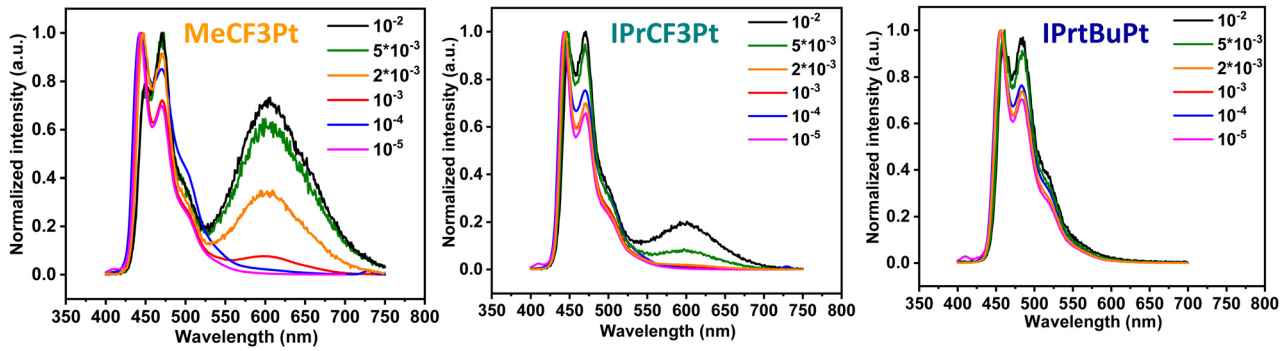

Fig. 2 Concentration-dependent PL spectra of the new Pt(II) complexes in DCM solution.

in lower photoluminescence quantum yields (PLQYs) compared to MeCF3Pt. Upon increasing the concentration from 10^{-5} to 10^{-2} M (Fig. 2), obvious excimer emission (peak at ~600 nm) is observed for MeCF3Pt and IPrCF3Pt. Notably, no such lower energy shoulder was observed for IPr*t*BuPt.

To better understand their photophysical properties, density functional theory (DFT) and time dependent-DFT (TD-DFT) calculations were carried out at the B3LYP/def2SVP level using the Gaussian16 program package.[43] As presented in Fig. 3, the highest occupied molecular orbitals (HOMOs) are localized on the central phenyl group of the pincer chelate and the Pt–Cl vector, while the lowest unoccupied molecular orbitals (LUMOs) are distributed over the whole molecules. Calculated HOMO and LUMO gaps followed an ascending order MeCF3Pt < IPrCF3Pt < IPr*t*BuPt, confirming the increasing electron-donating ability of alkyl substituents between the chelates (*i.e.*, CF3/Me to CF3/IPr then *t*Bu/IPr). As the HOMO–LUMO hopping account for over 80% of the lowest energy process, the transitions between S_0 and S_1/T_1 are consequently assigned to an admixture of MLCT/ILCT/XLCT (X denotes a halide), and with MLCT contributions being 12.9%, 11.5% and 11.8% for MeCF3Pt, IPrCF3Pt and IPr*t*BuPt (Table S1, ESI†), respectively. These percentages are considerably small compared to those of Pt(II) complexes documented in literature reports (*ca.* 20%),[44–46] which explains the relatively long radiative lifetimes of our Pt(II) carbene pincer emitters.

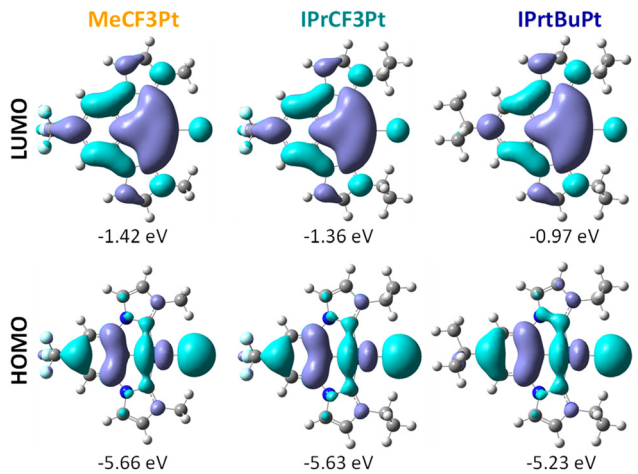

Fig. 3 Frontier molecular orbital distributions of MeCF3Pt, IPrCF3Pt and IPr*t*BuPt.

Single crystal analysis reveals that MeCF3Pt, IPrCF3Pt and IPr*t*BuPt possessed similar planar geometries but distinct packing behaviours. Selected bond lengths and angles are summarized in Table S2 (ESI†). The Pt–Cl, Pt–C_{ph} and Pt–C_{NHC} lengths are 2.38–2.41, 1.93–1.94 and 2.02–2.04 Å, respectively. The Cl–Pt–C_{Ph} and C_{NHC}–Pt–C_{NHC} bond angles were in the range of 177–179° and 156–158° respectively, presenting similar coordinating properties to other carbene Pt(II) pincer complexes in literature reports.[25,26] However, as shown in Fig. 4, intimately close Pt···Pt and π–π/Pt–π interactions are found in the unit cell of MeCF3Pt, confirming formation of excimers even at low doping concentrations. When the bulky *tert*-butyl group was added, only π–π interactions were observed, as indicated in the crystal cells of IPrCF3Pt. The addition of the *tert*-butyl group in IPr*t*BuPt also eliminated the respective face-to-face stacking interaction, explaining the photophysical properties observed earlier.

Before device fabrication, decomposition temperatures (T_d) of all studied complexes were analysed *via* thermogravimetric measurements (Fig. S1, ESI†) and all of them present good thermal stability with T_d exceeding 300 °C, indicating they are suitable for vacuum-deposition processes. These Pt(II) complexes were employed as dopant emitters with an OLED configuration of ITO/TAPC(20 nm)/TCTA(10 nm)/mCP(10 nm)/EML (20 nm)/3TPYMB(40 nm)/LiF(1 nm)/Al, in which bipolar mCPCN is employed as the host material in the EML. As presented in Fig. S2 (ESI†) and Table 2, being consistent in their packing properties, MeCF3Pt exhibited a broadened lower energy emission even at a doping level of 1 wt%. This excimer emission (peak at 597 nm, similar to the PL observed in doped thin films, excluding the contribution of the electromer, Fig. S3, ESI†) has gained intensity in comparison to the monomer emission (peak at 447 nm) *vs.* doping concentration dramatically. The higher intensity of long wavelength peak in EL (Fig. S2c, ESI†) compared to PL (Fig. S3, ESI†) revealed using EL spectra to detect the excimer signal is more sensitive and efficient. Its EQE_{max} was increased from 3.51 to 17.0%, which is ascribed to a favourable energy transfer from the host to the dopant and balanced carrier transport when doping concentration increased from 1 to 5 wt% and greater. Similarly, IPrCF3Pt exhibited excimer emissions starting from

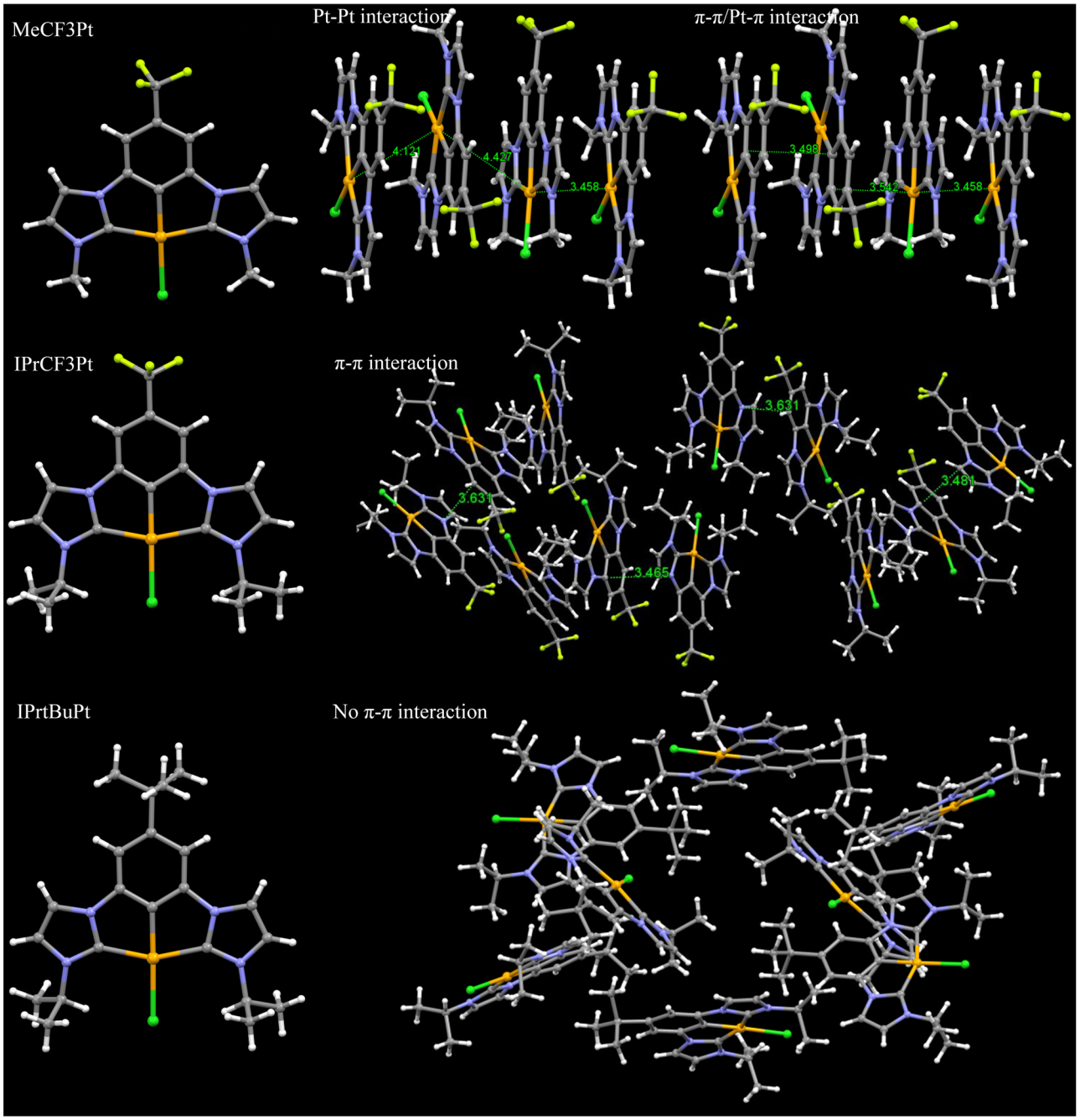

Fig. 4 Structure and intermolecular packing observed in single crystals of MeCF3Pt, IPrCF3Pt and IPr*t*BuPt.

8 wt% (Fig. S2f, ESI†). In sharp contrast, IPr*t*BuPt-based device displayed only higher energy, structured monomer emission even at 20 wt% (Fig. S2i, ESI†) and maintained a fairly stable CIE-*y* and EQE_{max} data of 0.221 and 12.38% @5 wt%, to 0.241 and 13.96% @20 wt%. However, the blue devices have low maximum brightness and show a dramatic efficiency roll-off with increased current density.

In view of its good resistance to excimer formation and good EL performance at high concentrations, IPr*t*BuPt was further employed as a dopant sensitizer for a narrow band MR-TADF terminal emitter: ν-DABNA. Importantly, the emission spectrum of IPr*t*BuPt shows a good overlap with the absorption spectrum of ν-DABNA. By integrating the overlap as shown in the ESI,† a large FRET radius of 7.1 nm (Fig. S4, ESI†) is estimated,[47,48] implying the potentially effective energy transfer processes. A hyperphosphorescent device with a configuration of ITO/HATCN/HATCN : TPAPB (3 : 7 30 nm)/TPAPB (10 nm)/PCzAc (10 nm)/16 wt% IPr*t*BuPt & 1 wt% ν-DABNA in mCBP : SiCzTrz 1 : 1 (30 nm)/DBFTrz (5 nm)/TmPyPB/LiF/Al was next fabricated. As shown in Fig. 5, a sharp EL profile peak at 471 nm and a narrow FWHM of 20 nm were achieved. EL spectra of the hyper device remained the same until high voltage (≥13 V), where the

Table 2 Summary of device performance of MeCF3Pt, IPrCF3Pt and IPr*t*BuPt with different doping ratios

Dopant	V_{on}[a] [V]	CE_{max}[b] [cd A^{-1}]	EQE_{max} [%]	CIE[c] [*x*, *y*]
MeCF3Pt 1 wt%	3.5	5.36	3.51	0.326, 0.26
MeCF3Pt 3 wt%	3.5	20.36	9.77	0.454, 0.363
MeCF3Pt 5 wt%	3.5	37.52	17.0	0.529, 0.419
IPrCF3Pt 5 wt%	3.5	5.29	5.03	0.163, 1.18
IPrCF3Pt 8 wt%	3.5	10.26	9.12	0.187, 0.138
IPrCF3Pt 10 wt%	3	17.39	13.3	0.191, 0.145
IPr*t*BuPt 5 wt%	3.5	20.48	12.38	0.153, 0.221
IPr*t*BuPt 10 wt%	3.5	23.2	13.93	0.156, 0.223
IPr*t*BuPt 20 wt%	3.0	24.26	13.96	0.159, 0.241

[a] Turn-on voltage at 1 cd m^{-2}. [b] Maximum current efficiency. [c] Recorded at 100 cd m^{-2}.

brightness was too high and pixels near the peaks were saturated (Fig. S5, ESI†). Impressively, a much-relieved roll-off with EQE_{max} and EQE_{1000} (EQE at 1000 cd m^{-2}) of 33.59 and 26.61%, respectively, comparable to the best hyper-OLED ever reported in the literature (Fig. S6, ESI†) were achieved.[7,8,15,24,30–34,36–38,49,50] However, the device lifetime of the hyper-device is only ~0.3 h (Fig. S7, ESI†), which may be attributed to the nucleophilic vulnerability of the Pt–Cl bond.

Conclusions

In summary, Pt(II) dicarbene pincer complexes were modified using different peripheral bulky substituents. The annoying issue of excimer formation for planar Pt(II) complexes is addressed by these peripheral groups, and blue emissions can be maintained even at a high concentration of 20 wt% in the doped device of IPr*t*BuPt. Notably, IPr*t*BuPt has successfully served as a dopant sensitizer for a *ν*-DABNA based hyper-OLED, giving max. EQE up to 33.59%, FWHM of 20 nm, and CIE coordinates of (0.124, 0.148). These results demonstrated a utilization of both the engineered emitters and smart device architecture to foster efficient blue OLED devices with mild efficiency roll-offs.

Experimental details

Synthesis

All solvents and reagents were purchased from commercial resources and used as received. All reactions were carried out in the air unless otherwise stated. Hexafluorophosphate salts of 1,3-bisimidazol-3-ium pro-chelates (denoted as $[(mimf)H_3{\cdot}(PF_6)_2]$, $[(pimf)H_3{\cdot}(PF_6)_2]$ and $[(pimb)H_3{\cdot}(PF_6)_2]$), namely 1,1′-(5-(trifluoromethyl)-1,3-phenylene)bis(3-methyl-1*H*-imidazol-3-ium), 1,1′-(5-(trifluoromethyl)-1,3-phenylene)bis(3-isopropyl-1*H*-imidazol-3-ium) and 1,1′-(5-(*tert*-butyl)-1,3-phenylene)bis(3-isopropyl-1*H*-imidazol-3-ium), were obtained using the method depicted in our previous report.[40,41]

Synthesis of the Pt(II) chlorides

A mixture of $[(mimf)H_3(PF_6)_2]$ (1.1 eq.), K_2PtCl_4 (1 eq.) and K_2CO_3 (10 eq.) was heated in refluxing propionic acid for 2 h. After cooled to RT, propionic acid was evaporated and the residue was dissolved in CH_2Cl_2. The solution was washed with deionized water, dried over anhydrous Na_2SO_4, filtered and concentrated to dryness. The crude product was purified by silica gel column chromatography, eluting with a (1 : 4) mixture of ethyl acetate and hexane to afford the targeted Pt(II) carbene pincer complexes.

Spectral data of MeCF3Pt. ^{1}H NMR (400 MHz, $CDCl_3$, 296 K): δ 7.37 (d, J = 2.0 Hz, 2H), 7.06 (s, J_{PtH} = 16.8 Hz, 2H), 6.98 (d, J = 2.0 Hz, 2H), 4.26 (s, 6H); ^{19}F NMR (376 MHz, $CDCl_3$, 296 K): δ −61.17 (s, 3F). HRMS (Q-TOF) *m*/*z* for $[M - Cl]^+$ calcd 500.0657, found 500.0639.

Spectral data of IPrCF3Pt. ^{1}H NMR (400 MHz, $CDCl_3$, 296 K): δ 7.43 (d, J = 2.0 Hz, 2H), 7.14 (d, J = 2.0 Hz, 2H), 7.12 (s, J_{PtH} = 19.2 Hz, 2H), 6.18 (q, J = 6.8 Hz, 2H), 1.52 (d, J = 6.8 Hz, 12H); ^{19}F NMR (376MHz, $CDCl_3$, 296 K): δ −61.22 (s, 3F). HRMS (Q-TOF) *m*/*z* for $[M - Cl]^+$ calcd 556.1283, found 556.1272.

Spectral data of IPr*t*BuPt. ^{1}H NMR (400 MHz, $CDCl_3$, 296 K): δ 7.39 (d, J = 2.0 Hz, 2H), 7.07 (d, J = 2.0 Hz, 2H), 6.90 (s, J_{PtH} = 16.0 Hz, 2H), 6.15 (q, J = 6.8 Hz, 2H), 1.50 (d, J = 6.8 Hz, 12H), 1.36 (s, 9H). HRMS (Q-TOF) *m*/*z* for $[M - Cl]^+$ calcd 544.2040, found 544.2020.

Author contributions

Y. C. and C. S. L. initiated and provided financial support for the project. Y. C. designed the complexes. J. Y., Z. L. Z. and L.W. F. synthesized and characterized the new molecules. Y. J, C. C. and Z. L. Z. carried out photophysical measurements. J. H. T performed the computational calculation under the

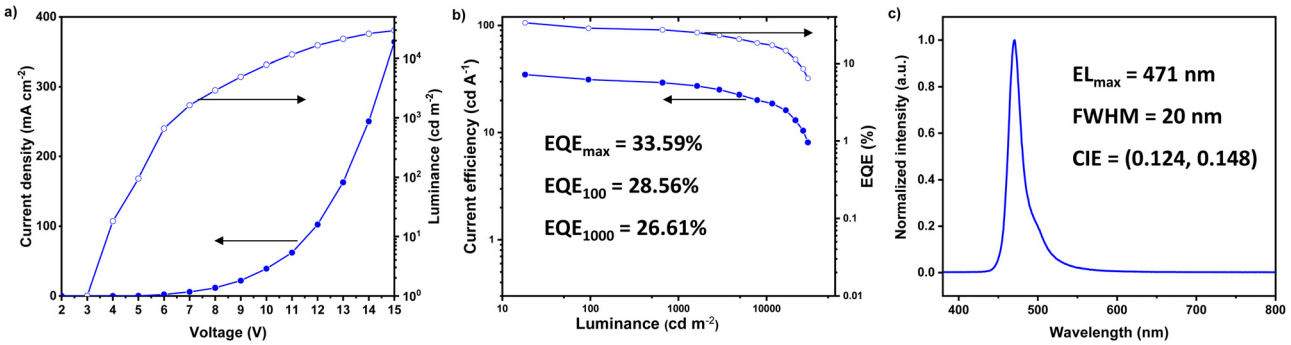

Fig. 5 (a) Current density–voltage–luminance plots, (b) current efficiency–luminance–EQE curves and (c) EL spectrum of an IPr*t*BuPt based hyper-OLED.

supervision of Z. L. Z. J. Y. and Z. L. Z. contributed to crystal growth and crystal data analysis. Z. L. Z. fabricated the OLEDs and measured the device performance. Y. J. and Z.L. Z. wrote the first draft. Z. L. Z., Y. C. and C.S. L. provided suggestions on experiments, revised manuscript and supervised the project. All authors discussed the experimental result and reviewed the manuscript.

Conflicts of interest

There are no conflicts to declare.

Acknowledgements

C. S. L. is thankful for the financial support from the Research Grants Council of the Hong Kong Special Administrative Region, China (Project No. C1009-17E, CityU 11300320 and N_CityU104/20). Y. C. is supported by the Research Grants Council funding: CityU 11304221 and CityU 11312722.

Notes and references

1 Y. Im, S. Y. Byun, J. H. Kim, D. R. Lee, C. S. Oh, K. S. Yook and J. Y. Lee, Recent Progress in High-Efficiency Blue-Light-Emitting Materials for Organic Light-Emitting Diodes, *Adv. Funct. Mater.*, 2017, **27**, 1603007.

2 S. K. Jeon, H. L. Lee, K. S. Yook and J. Y. Lee, Recent Progress of the Lifetime of Organic Light-Emitting Diodes Based on Thermally Activated Delayed Fluorescent Material, *Adv. Mater.*, 2019, **31**, 1803524.

3 A. Maheshwaran, V. G. Sree, H.-Y. Park, H. Kim, S. H. Han, J. Y. Lee and S.-H. Jin, High Efficiency Deep-Blue Phosphorescent Organic Light-Emitting Diodes with CIE x, y ($\leq$0.15) and Low Efficiency Roll-Off by Employing a High Triplet Energy Bipolar Host Material, *Adv. Funct. Mater.*, 2018, **28**, 1802945.

4 A. K. Pal, S. Krotkus, M. Fontani, C. F. R. Mackenzie, D. B. Cordes, A. M. Z. Slawin, I. D. W. Samuel and E. Zysman-Colman, High-Efficiency Deep-Blue-Emitting Organic Light-Emitting Diodes Based on Iridium(III) Carbene Complexes, *Adv. Mater.*, 2018, **30**, 1804231.

5 H.-Y. Park, A. Maheshwaran, C.-K. Moon, H. Lee, S. S. Reddy, V. G. Sree, J. Yoon, J. W. Kim, J. H. Kwon, J.-J. Kim and S.-H. Jin, External Quantum Efficiency Exceeding 24% with CIEy Value of 0.08 using a Novel Carbene-Based Iridium Complex in Deep-Blue Phosphorescent Organic Light-Emitting Diodes, *Adv. Mater.*, 2020, **32**, 2002120.

6 A. Monkman, Why Do We Still Need a Stable Long Lifetime Deep Blue OLED Emitter?, *ACS Appl. Mater. Interfaces*, 2021, **14**, 20463.

7 J. Jin, Z. Zhu, J. Yan, X. Zhou, C. Cao, P.-T. Chou, Y.-X. Zhang, Z. Zheng, C.-S. Lee and Y. Chi, Iridium(III) Phosphors–Bearing Functional 9-Phenyl-7,9-dihydro-8H-purin-8-ylidene Chelates and Blue Hyperphosphorescent OLED Devices, *Adv. Photonics Res.*, 2022, **3**, 2100381.

8 Z.-L. Zhu, P. Gnanasekaran, J. Yan, Z. Zheng, C.-S. Lee, Y. Chi and X. Zhou, Efficient Blue Electrophosphorescence and Hyperphosphorescence Generated by Bis-tridentate Iridium(III) Complexes, *Inorg. Chem.*, 2022, **61**, 8898.

9 T. Hatakeyama, K. Shiren, K. Nakajima, S. Nomura, S. Nakatsuka, K. Kinoshita, J. Ni, Y. Ono and T. Ikuta, Ultrapure Blue Thermally Activated Delayed Fluorescence Molecules: Efficient HOMO–LUMO Separation by the Multiple Resonance Effect, *Adv. Mater.*, 2016, **28**, 2777.

10 M. Yang, I. S. Park and T. Yasuda, Full-Color, Narrowband, and High-Efficiency Electroluminescence from Boron and Carbazole Embedded Polycyclic Heteroaromatics, *J. Am. Chem. Soc.*, 2020, **142**, 19468.

11 Y. Yuan, X. Tang, X.-Y. Du, Y. Hu, Y.-J. Yu, Z.-Q. Jiang, L.-S. Liao and S.-T. Lee, The Design of Fused Amine/Carbonyl System for Efficient Thermally Activated Delayed Fluorescence: Novel Multiple Resonance Core and Electron Acceptor, *Adv. Opt. Mater.*, 2019, **7**, 1801536.

12 A. Hofmann, M. Schmid and W. Brütting, The Many Facets of Molecular Orientation in Organic Optoelectronics, *Adv. Opt. Mater.*, 2021, **9**, 2101004.

13 H. J. Kim and T. Yasuda, Narrowband Emissive Thermally Activated Delayed Fluorescence Materials, *Adv. Opt. Mater.*, 2022, **10**, 2201714.

14 X.-C. Fan, K. Wang, Y.-Z. Shi, Y.-C. Cheng, Y.-T. Lee, J. Yu, X.-K. Chen, C. Adachi and X.-H. Zhang, Ultrapure green organic light-emitting diodes based on highly distorted fused π-conjugated molecular design, *Nat. Photonics*, 2023, **17**, 280–285.

15 Y. Kondo, K. Yoshiura, S. Kitera, H. Nishi, S. Oda, H. Gotoh, Y. Sasada, M. Yanai and T. Hatakeyama, Narrowband deep-blue organic light-emitting diode featuring an organoboron-based emitter, *Nat. Photonics*, 2019, **13**, 678.

16 Y.-C. Cheng, X.-C. Fan, F. Huang, X. Xiong, J. Yu, K. Wang, C.-S. Lee and X.-H. Zhang, A Highly Twisted Carbazole-Fused DABNA Derivative as an Orange-Red TADF Emitter for OLEDs with Nearly 40% EQE, *Angew. Chem., Int. Ed.*, 2022, **134**, e202212575.

17 Y. X. Hu, J. Miao, T. Hua, Z. Huang, Y. Qi, Y. Zou, Y. Qiu, H. Xia, H. Liu, X. Cao and C. Yang, Efficient selenium-integrated TADF OLEDs with reduced roll-off, *Nat. Photonics*, 2022, **16**, 803.

18 G. Ni, J. Yan, Y. Wu, F. Zhou, P.-T. Chou and Y. Chi, Transition-metal phosphors with emission peak maximum on and beyond the visible spectral boundaries, *Inorg. Chem. Front.*, 2023, **10**, 1395.

19 R. Kumaresan, H.-Y. Park, A. Maheshwaran, H. Park, Y. Do, M. Song, J. Yoon, S. I. Ahn and S.-H. Jin, High Performance Solution-Processed Deep-Blue Phosphorescence Organic Light-Emitting Diodes with EQE Over 24% by Employing New Carbenic Ir(III) Complexes, *Adv. Opt. Mater.*, 2021, **10**, 2101686.

20 S. L. Murov, I. Carmichael and G. L. Hug, *Handbook of photochemistry*, CRC Press, 1993.

21 T. Fleetham, G. Li and J. Li, Phosphorescent Pt(II) and Pd(II) Complexes for Efficient, High-Color-Quality, and Stable OLEDs, *Adv. Mater.*, 2017, **29**, 1601861.

22 T. Fleetham, G. Li, L. Wen and J. Li, Efficient ''Pure'' Blue OLEDs Employing Tetradentate Pt Complexes with a Narrow Spectral Bandwidth, *Adv. Mater.*, 2014, **26**, 7116.
23 J. Liu, T.-L. Lam, M.-K. Sit, Q. Wan, C. Yang, G. Cheng and C.-M. Che, Pure blue phosphorescent platinum(II) emitters supported by NHC-based pincer type ligands with unitary emission quantum yields, *J. Mater. Chem. C*, 2022, **10**, 10271.
24 K.-W. Lo, G. S. M. Tong, G. Cheng, K.-H. Low and C.-M. Che, Dinuclear PtII Complexes with Strong Blue Phosphorescence for Operational Stable Organic Light-Emitting Diodes with EQE up to 23% at 1000 cd m^{-2}, *Angew. Chem., Int. Ed.*, 2022, **61**, e202115515.
25 T. Fleetham, Z. Wang and J. Li, Efficient deep blue electrophosphorescent devices based on platinum(II) bis(n-methylimidazolyl)benzene chloride, *Org. Electron.*, 2012, **13**, 1430.
26 X. Zhang, A. M. Wright, N. J. DeYonker, T. K. Hollis, N. I. Hammer, C. E. Webster and E. J. Valente, Synthesis, Air Stability, Photobleaching, and DFT Modeling of Blue Light Emitting Platinum CCC-N-Heterocyclic Carbene Pincer Complexes, *Organometallics*, 2012, **31**, 1664.
27 M. A. Baldo, M. E. Thompson and S. R. Forrest, High-efficiency fluorescent organic light-emitting devices using a phosphorescent sensitizer, *Nature*, 2000, **403**, 750.
28 D. Zhang, L. Duan, Y. Li, H. Li, Z. Bin, D. Zhang, J. Qiao, G. Dong, L. Wang and Y. Qiu, Towards High Efficiency and Low Roll-Off Orange Electrophosphorescent Devices by Fine Tuning Singlet and Triplet Energies of Bipolar Hosts Based on Indolocarbazole/1, 3, 5-Triazine Hybrids, *Adv. Funct. Mater.*, 2014, **24**, 3551.
29 *Thermally activated delayed fluorescence organic light-emitting diodes (TADF-OLEDs)*, ed. L. Duan, Woodhead Publishing, An imprint of Elsevier, Duxford, DK Cambridge, MA Kidlington, OX, 2022.
30 R. Braveenth, H. Lee, J. D. Park, K. J. Yang, S. J. Hwang, K. R. Naveen, R. Lampande and J. H. Kwon, Achieving Narrow FWHM and High EQE Over 38% in Blue OLEDs Using Rigid Heteroatom-Based Deep Blue TADF Sensitized Host, *Adv. Funct. Mater.*, 2021, **31**, 2105805.
31 D. Zhang, Y. Wada, Q. Wang, H. Dai, T. Fan, G. Meng, J. Wei, Y. Zhang, K. Suzuki, G. Li, L. Duan and H. Kaji, Highly Efficient and Stable Blue Organic Light-Emitting Diodes based on Thermally Activated Delayed Fluorophor with Donor-Void-Acceptor Motif, *Adv. Sci.*, 2022, 2106018.
32 S. O. Jeon, K. H. Lee, J. S. Kim, S.-G. Ihn, Y. S. Chung, J. W. Kim, H. Lee, S. Kim, H. Choi and J. Y. Lee, High-efficiency, long-lifetime deep-blue organic light-emitting diodes, *Nat. Photonics*, 2021, **15**, 208.
33 C.-Y. Chan, M. Tanaka, Y.-T. Lee, Y.-W. Wong, H. Nakanotani, T. Hatakeyama and C. Adachi, Stable pure-blue hyperfluorescence organic light-emitting diodes with high-efficiency and narrow emission, *Nat. Photonics*, 2021, **15**, 203.
34 T. Huang, Q. Wang, G. Meng, L. Duan and D. Zhang, Accelerating Radiative Decay in Blue Through-Space Charge Transfer Emitters by Minimizing the Face-to-Face Donor–Acceptor Distances, *Angew. Chem., Int. Ed.*, 2022, **134**, e202200059.
35 K. Stavrou, A. Danos, T. Hama, T. Hatakeyama and A. Monkman, Hot Vibrational States in a High-Performance Multiple Resonance Emitter and the Effect of Excimer Quenching on Organic Light-Emitting Diodes, *ACS Appl. Mater. Interfaces*, 2021, **13**, 8643.
36 W. J. Chung, K. H. Lee, M. Jung, K. M. Lee, H. C. Park, M.-S. Eum and J. Y. Lee, Over 30 000 h Device Lifetime in Deep Blue Organic Light-Emitting Diodes with y Color Coordinate of 0.086 and Current Efficiency of 37.0 cd A^{-1}, *Adv. Opt. Mater.*, 2021, **9**, 2100203.
37 M. Mamada, H. Katagiri, C.-Y. Chan, Y.-T. Lee, K. Goushi, H. Nakanotani, T. Hatakeyama and C. Adachi, Highly Efficient Deep-Blue Organic Light-Emitting Diodes Based on Rational Molecular Design and Device Engineering, *Adv. Funct. Mater.*, 2022, **32**, 2204352.
38 S. Nam, J. W. Kim, H. J. Bae, Y. M. Maruyama, D. Jeong, J. Kim, J. S. Kim, W.-J. Son, H. Jeong, J. Lee, S.-G. Ihn and H. Choi, Improved Efficiency and Lifetime of Deep-Blue Hyperfluorescent Organic Light-Emitting Diode using Pt(II) Complex as Phosphorescent Sensitizer, *Adv. Sci.*, 2021, **8**, 2100586.
39 C.-Y. Kuei, W.-L. Tsai, B. Tong, M. Jiao, W.-K. Lee, Y. Chi, C.-C. Wu, S.-H. Liu, G.-H. Lee and P.-T. Chou, Bis-Tridentate Ir(III) Complexes with Nearly Unitary RGB Phosphorescence and Organic Light-Emitting Diodes with External Quantum Efficiency Exceeding 31%, *Adv. Mater.*, 2016, **28**, 2795.
40 Z.-L. Zhu, L.-Y. Hsu, W.-S. Tai, S.-F. Ni, C.-S. Lee and Y. Chi, Revealing the role of 1,2,4-triazolate fragment of blue-emitting bis-tridentate Ir(III) phosphors: photophysical properties, photo-stabilities, and applications, *Mater. Today Energy*, 2021, **20**, 100636.
41 Z.-L. Zhu, W.-C. Chen, S.-F. Ni, J. Yan, S. F. Wang, L.-W. Fu, H.-Y. Tsai, Y. Chi and C.-S. Lee, Constructing deep-blue bis-tridentate Ir(III) phosphors with fluorene-based dianionic chelates, *J. Mater. Chem. C*, 2021, **9**, 1318.
42 J. Li, P. I. Djurovich, B. D. Alleyne, M. Yousufuddin, N. N. Ho, J. C. Thomas, J. C. Peters, R. Bau and M. E. Thompson, Synthetic Control of Excited-State Properties in Cyclometalated Ir(III) Complexes Using Ancillary Ligands, *Inorg. Chem.*, 2005, **44**, 1713.
43 M. J. Frisch, G. W. Trucks, H. B. Schlegel, G. E. Scuseria, M. A. Robb, J. R. Cheeseman, G. Scalmani, V. Barone, G. A. Petersson, H. Nakatsuji, X. Li, M. Caricato, A. V. Marenich, J. Bloino, B. G. Janesko, R. Gomperts, B. Mennucci, H. P. Hratchian, J. V. Ortiz, A. F. Izmaylov, J. L. Sonnenberg Williams, F. Ding, F. Lipparini, F. Egidi, J. Goings, B. Peng, A. Petrone, T. Henderson, D. Ranasinghe, V. G. Zakrzewski, J. Gao, N. Rega, G. Zheng, W. Liang, M. Hada, M. Ehara, K. Toyota, R. Fukuda, J. Hasegawa, M. Ishida, T. Nakajima, Y. Honda, O. Kitao, H. Nakai, T. Vreven, K. Throssell, J. A. Montgomery Jr., J. E. Peralta, F. Ogliaro, M. J. Bearpark, J. J. Heyd, E. N. Brothers, K. N. Kudin, V. N. Staroverov, T. A. Keith, R. Kobayashi, J. Normand, K. Raghavachari, A. P. Rendell, J. C. Burant, S. S. Iyengar, J. Tomasi, M. Cossi, J. M. Millam, M. Klene, C. Adamo,

R. Cammi, J. W. Ochterski, R. L. Martin, K. Morokuma, O. Farkas, J. B. Foresman and D. J. Fox, *Gaussian 16, Rev. C.01*, 2016.

44 Z.-L. Zhu, S.-F. Wang, L.-W. Fu, J.-H. Tan, C. Cao, Y. Yuan, S.-M. Yiu, Y.-X. Zhang, Y. Chi and C.-S. Lee, Efficient Pyrazolo[5,4-*f*]quinoxaline Functionalized Os(II) based Emitter with Electroluminescence Peak Maximum at 811 nm, *Chem. – Eur. J.*, 2022, **28**, e202103202.

45 L.-M. Huang, G.-M. Tu, Y. Chi, W.-Y. Hung, Y.-C. Song, M.-R. Tseng, P.-T. Chou, G.-H. Lee, K.-T. Wong, S.-H. Cheng and W.-S. Tsai, Mechanoluminescent and efficient white OLEDs for Pt(II) phosphors bearing spatially encumbered pyridinyl pyrazolate chelates, *J. Mater. Chem. C*, 2013, **1**, 7582.

46 K.-Y. Liao, C.-W. Hsu, Y. Chi, M.-K. Hsu, S.-W. Wu, C.-H. Chang, S.-H. Liu, G.-H. Lee, P.-T. Chou, Y. Hu and N. Robertson, Pt(II) Metal Complexes Tailored with a Newly Designed Spiro-Arranged Tetradentate Ligand; Harnessing of Charge-Transfer Phosphorescence and Fabrication of Sky Blue and White OLEDs, *Inorg. Chem.*, 2015, **54**, 4029.

47 C. Zhang, Y. Lu, Z. Liu, Y. Zhang, X. Wang, D. Zhang and L. Duan, A π–D and π–A Exciplex-Forming Host for High-Efficiency and Long-Lifetime Single-Emissive-Layer Fluorescent White Organic Light-Emitting Diodes, *Adv. Mater.*, 2020, **32**, 2004040.

48 N. Hildebrandt and I. L. Medintz, *FRET-Forster Resonance Energy Transfer: From Theory to Applications*, Wiley-VCH Verlag GmbH, 2014.

49 D. Zhou, S. Wu, G. Cheng and C.-M. Che, A gold(III)–TADF emitter as a sensitizer for high-color-purity and efficient deep-blue solution-processed OLEDs, *J. Mater. Chem. C*, 2022, **10**, 4590.

50 K. J. Yang, H. Lee, R. Braveenth, S. J. Hwang, S. J. Kim and J. H. Kwon, Analysis of efficiency variations in ν-DABNA based thermally activated delayed fluorescence OLED devices, *J. Ind. Eng. Chem.*, 2022, **108**, 47.